International Journal of Nanomedicine

Dovepress
open access to scientific and medical research

Open Access Full Text Article

ORIGINAL RESEARCH

Anticancer Evaluation of Methoxy Poly(Ethylene Glycol)-*b*-Poly(Caprolactone) Polymeric Micelles Encapsulating Fenbendazole and Rapamycin in Ovarian Cancer

Yu Been Shin[1,*], Ju-Yeon Choi[2,*], Dae Hwan Shin[1], Jeong-Won Lee[2,3]

[1]College of Pharmacy, Chungbuk National University, Cheongju, 28160, Republic of Korea; [2]Research Institute for Future Medicine, Samsung Medical Center, Sungkyunkwan University School of Medicine, Seoul, South Korea; [3]Department of Obstetrics and Gynecology, Samsung Medical Center, Sungkyunkwan University School of Medicine, Seoul, South Korea

*These authors contributed equally to this work

Correspondence: Dae Hwan Shin, College of Pharmacy, Chungbuk National University, Osongsaengmyeong 1-ro, Osong-eup, Heungdeok-gu, Cheongju, 28160, Republic of Korea, Tel +82 43 261 2820, Fax +82 43 268 2732, Email dshin@chungbuk.ac.kr; Jeong-Won Lee, Department of Obstetrics and Gynecology, Samsung Medical Center, Sungkyunkwan University School of Medicine, 81, Irwon-ro, Gangnam-gu, Seoul, 06351, South Korea, Tel +82-2-3410-1382, Fax +82-2-3410-0630, Email garden.lee@samsung.com

Purpose: We aimed to inhibit ovarian cancer (OC) development by interfering with microtubule polymerization and inhibiting mTOR signaling. To achieve this, previously developed micelles containing fenbendazole and rapamycin were applied.

Methods: Herein, we prepared micelles for drug delivery using fenbendazole and rapamycin at a 1:2 molar ratio and methoxy poly (ethylene glycol)-*b*-poly(caprolactone)(mPEG-*b*-PCL) via freeze-drying. We revealed their long-term storage capacity of up to 120 days. Furthermore, a cytotoxicity test was performed on the OC cell line HeyA8, and an orthotopic model was established for evaluating in vivo antitumor efficacy.

Results: Fenbendazole/rapamycin-loaded mPEG-*b*-PCL micelle (M-FR) had an average particle size of 37.2 ± 1.10 nm, a zeta potential of −0.07 ± 0.09 mV, and a polydispersity index of 0.20 ± 0.02. Additionally, the average encapsulation efficiency of fenbendazole was 75.7 ± 4.61% and that of rapamycin was 98.0 ± 1.97%. In the clonogenic assay, M-FR was 6.9 times more effective than that free fenbendazole/rapamycin. The in vitro drug release profile showed slower release in the combination formulation than in the single formulation.

Conclusion: There was no toxicity, and tumor growth was suppressed substantially by our formulation compared with that seen with the control. The findings of our study lay a foundation for using fenbendazole and rapamycin for OC treatment.

Keywords: ovarian cancer treatment, combination therapy, drug delivery, nanoformulation

Introduction

Ovarian cancer (OC) is the deadliest gynecological cancer,[1,2] distinguished into epithelial ovarian cancer (EOC) and non-epithelial ovarian cancer.[3] Although several treatments, such as targeted therapy, chemotherapy, and surgery, have been developed to treatment of EOC, side effects and sequelae still occur.[4–7] To overcome this challenge, drug delivery using nanocarriers is a promising treatment method to maximize the efficacy and stability of drugs.[8–11] Nanocarriers deliver poorly soluble drugs,[12,13] and increase the residence time in the body,[9,14–16] thereby maximizing the therapeutic efficacy.[17–21] In particular, the drug encapsulated in nanocarriers can be designed to accumulate adequately in the tumor using the enhanced permeability and retention (EPR) effect.[22–25] Solvents as such as polysorbate 80 (Tween 80®), Cremophor EL® and ethanol are used to dissolve poorly soluble drugs in intravenous formulations, but these have side effects and toxicity due to the toxicity of the solvent.[26,27] These disadvantages can also be overcome with nanocarriers.

Received: 24 October 2022
Accepted: 25 January 2023
Published: 1 May 2023

Therefore, we designed micelles using methoxy poly(ethylene glycol)-*b*-poly(caprolactone) (mPEG-*b*-PCL) polymer in a simple way. Poly(caprolactone) (PCL) is a biodegradable, biocompatible, and semi-crystalline polymer with a very low glass transition temperature,[28] which has been used as nanoparticles encapsulated with anticancer agents.[28,29] Poly(ethylene glycol) (PEG) is hydrophilic, non-toxic, and non-immunogenic.[30] PEGylation of hydrophobic nanoparticles offers advantages such as amphiphilicity, improved biocompatibility, and controllable degradation rates. As such, micelles formed using mPEG-*b*-PCL show biodegradability, biocompatibility, amphiphilicity, blood stability, non-toxicity, non-immunogenicity, and non-inflammatory properties,[31] and have been used as an excellent drug delivery system.[32,33]

Combination therapy using two or more drugs has many benefits. By administering a combination of two drugs acting via different molecular mechanisms, individual compound doses can be reduced to minimize or lower drug toxicity.[34,35] In addition, it can reduce the likelihood of drug resistance arising from continued treatment with a single drug.[36] Finally, if the formulation is designed using a rational drug combination, it can further help inhibit cancer cells.[37]

Owing to its low toxicity and side effects and high safety in several experimental animal models, fenbendazole is a broad-spectrum benzimidazole anthelmintic approved for use in many animals.[38–41] Currently, widely used anticancer drugs such as paclitaxel and docetaxel exhibit antitumor effects by interfering with microtubule polymerization and formation.[42,43] Fenbendazole interferes with microtubule polymerization and blocks cell cycle progression.[44,45] In addition, the mechanism of anticancer activity of fenbendazole occurs through increased p53 protein stability and apoptosis induction.[46] While developing new drugs is time-consuming and expensive, repurposing drugs is a promising efficient and economical alternative.[47] Fenbendazole, an antiparasitic drug with potential for anticancer activity,[48] such as apoptosis, microtubule inhibition, and inhibition of cancer cell invasion and migration, can be a promising anticancer agent.[49–52] However, fenbendazole has low permeability and water solubility; hence, its bioavailability is low.[53,54]

Rapamycin is a well-known potent immunosuppressant which inhibits the function of the mammalian target of rapamycin (mTOR)[55] and angiogenesis.[56,57] Hence, rapamycin can be expected to have excellent anticancer effects.[58,59] The mTOR signaling pathway plays an important role in cell survival, growth, proliferation, and angiogenesis.[60,61] Furthermore, abnormalities in the mTOR pathway cause tumorigenesis, such as OC.[62,63] Several preclinical models have been developed to demonstrate the role of the mTOR signaling pathway in OC.[64] Another study demonstrated the efficacy of an OC model for preclinical testing of inhibitors of mTOR signaling.[65] When mTOR is targeted, it significantly inhibits OC cell proliferation and migration.[66] The combination of a drug that interferes with microtubule polymerization and an mTOR inhibitor has a synergistic effect.[67] Despite being efficient, rapamycin has the disadvantage of low bioavailability and water solubility (2.6 μg/mL).[68,69]

To increase the bioavailability of poorly soluble drugs, a method of encapsulating the drug in a polymer and delivering it into the body is widely used.[70,71] Many studies have developed drug delivery systems that can control the release time of rapamycin and prolong its residence time in the body.[72] Moreover, successful delivery via intravenous (IV) injection of these formulations has been reported.[73] To improve the bioavailability of fenbendazole and rapamycin and maximize their anticancer potential, we demonstrated an IV formulation in micelles.

In this study, fenbendazole/rapamycin-loaded micelles (M-FR) were evaluated for EOC treatment. We evaluated the synergism of the two drugs in OC, their formulation stability, and long-term storage capacity. We estimated their cytotoxicity using EOC cell line HeyA8, performed an in vitro release assay, and antitumor efficacy in vivo. The anticancer effect of mPEG-*b*-PCL micelles in combination with fenbendazole and rapamycin has been demonstrated in lung cancer.[74] Here, we evaluated the anticancer ability of this formulation in OC and established an orthotopic model to further observe its anticancer activity in the body. We believe that this study will be of great help in the development of OC treatments.

Materials and Methods

Materials and Reagents

Acetonitrile (ACN) and Hanks' Balanced Salt Solution (HBSS) were purchased from Thermo Fisher Scientific (Waltham, MA, USA). Distilled water (DW) was purchased from Tedia (Fairfield, OH, USA). Rapamycin was purchased

from LC Laboratories® (Woburn, MA, USA). Thiazolyl blue tetrazolium bromide (MTT), *tert*-Butyl alcohol, dimethyl sulfoxide (DMSO), and fenbendazole were purchased from Sigma-Aldrich Corp. (St. Louis, MO, USA). The mPEG-*b*-PCL (MW~2000:2000 Da) was purchased from PolySciTech® (West Lafayette, IN, USA). All other reagents were of analytical reagent grade.

High-Performance Liquid Chromatography (HPLC) Analysis

The concentrations of fenbendazole and rapamycin in the samples were analyzed using a Waters HPLC system (Milford, MA, USA) consisting of a 2695 separation module and a 2996 photodiode array detector. A Fortis C18 chromatography column (5 μm, 4.6×250 mm) was used at 30°C for analysis. Fenbendazole and rapamycin were eluted in the isocratic mode; the injection volume was 10 μL, and the flow rate of the mobile phase consisting of ACN/DW (70:30, v/v) was 1.0 mL/min. Fenbendazole was detected at 295 nm, and the retention time was 5 min. Rapamycin was detected at 277 nm, with a retention time of 20 min. The concentration of each drug was calculated by comparing the calibration curve to the peak area.

Cell Lines and Cell Culture

Human OC (HeyA8_RRID: CVCL8878) cells were a gift from Dr. Anil K. Sood, Department of Cancer Biology, University of Texas M.D. Anderson Cancer Center, TX, USA. Penicillin streptomycin solution, fetal bovine serum (FBS), Roswell Park Memorial Institute 1640 (RPMI 1640) medium, Dulbecco's phosphate-buffered saline (DPBS) and trypsin were purchased from Corning Inc. (Corning, NY, USA). HeyA8 cells were cultured in the RPMI 1640 medium supplemented with 1% (w/v) penicillin streptomycin solution and 10% (v/v) FBS. Cells were grown at 37°C under a 5% CO_2 atmosphere.

Preparation of Micelles

M-FR were prepared using the freeze-drying method (Figure 1).[74] Briefly, the polymer and various ratios of fenbendazole and rapamycin were weighed in a scintillation vial and dissolved in 1 mL *tert*-butanol at 60°C. After adding 1 mL DW at 60°C, the solution was vortexed. The samples were stored in a −70°C freezer for 1 h and then lyophilized (Advantage Pro; SP Scientific, Warminster, PA, USA) at −20°C for 24 h. For reconstitution, 1 mL of 60°C DW was added to the freeze-dried cake, and vortexed. After centrifugation (Hanil Science Inc., Gimpo, South Korea) at 4°C and 13,000 rpm for 5 min, unencapsulated drugs and polymers were removed, and the centrifuged micelle supernatant was filtered with a 0.2 μm-pore size filter (Corning, NY, USA).

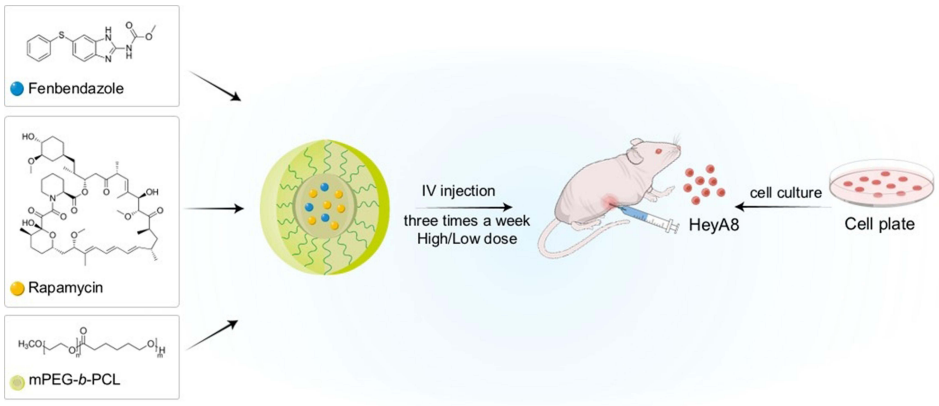

Figure 1 Schematic diagram of cell injection for orthotopic model establishment and M-FR IV injection for OC treatment.

Physicochemical Characterization of the Micelles

All particle size, zeta potential, and polydispersity index (PDI) measured using a dynamic light scattering (DLS) device (Litesizer 500, Anton Paar, Graz, Austria). All samples were diluted 10 times with DW before measurement.

The encapsulation efficiency (EE, %) and drug loading (DL, %) of fenbendazole and rapamycin in this study were measured using HPLC and calculated as follows:[75,76]

$$\mathrm{EE}(\%) = \frac{\text{Weight of drug in micelles}}{\text{Weight of feeding drug}} \times 100$$

$$\mathrm{DL}(\%) = \frac{\text{Weight of drug in micelles}}{\text{Weight of feeding drug and polymer}} \times 100$$

The results of each micelle sample analysis were expressed as the mean ± SD of three separate experiments.

The morphology of M-FR was observed by using a JEM-2100 transmission electron microscope (TEM, JEOL LTD., Tokyo, Japan). In the sample preparation procedure for TEM measurement, the diluted micelle solution was dropped on a copper grid, dried at room temperature for 2 days, and examined at accelerating voltage of 200 Kv.

Analysis of the Combination Index (CI) Between Drugs

CI was analyzed using Chou's method to analyze interactions between drugs.[77] The CI value between fenbendazole and rapamycin was calculated using the following equation:

$$\text{Combination Index (CI)} = \frac{(D)_1}{(D_x)_2} + \frac{(D)_2}{(D_x)_2}$$

$(D_x)_1$ and $(D_x)_2$ in this equation are the inhibitory concentrations of drugs 1 and 2, respectively. $(D)_1$ and $(D)_2$ are the inhibitory concentrations of each drug in combinations. CI < 1 indicated synergism, CI > 1 indicated antagonism, and CI = 1 indicated an additive effect.

M-FR Stability Test

M-FR stability was tested in a refrigerator at 4°C and in a water bath 37°C. On days 0, 1, 2, 4, 7, 10, and 14, 100 μL of each sample was collected and dissolved in 900 μL DW for measurement. The size and PDI of M-FR were measured using a DLS device. The experiments were conducted in triplicate.

Storage Stability Test After Freeze-Drying

All M-FR required for the experiment were prepared at once on the same day, and the freeze-dried M-FR were stored in a −20°C freezer until testing. M-FR were hydrated on days 1, 7, 14, 30, 60 and 120 to measured EE (%), size, PDI and zeta potential. Based on this, the possibility of long-term storage use was evaluated. This experiment was performed three times.

In vitro Cytotoxicity Assay

Cytotoxicity was performed by MTT assay.[78] HeyA8 cells were seeded at 4000 cells/well in a 96-well plate, and incubated at 37°C and 5% CO_2 conditions for 24 h. Then, the medium was replaced with a fresh medium with varying molar ratios of free fenbendazole/rapamycin, free fenbendazole, free rapamycin or M-FR each. A medium without any drug was used as the control (CON). The cells treated with various drug combinations and M-FR were incubated for 48 h. The treated high concentrations of free fenbendazole and free rapamycin were 170,000 nM and 54,705 nM, respectively, which were diluted 10-fold. The medium was removed, and 100 μL of MTT solution (0.5 mg/mL) was added and incubated for 4 h. The MTT solution was removed and 100 μL of DMSO was added, followed by shaking for 10 min using an orbital shaker (NB-101S; N-BIOTEK, Bucheon, South Korea) at 200 rpm for complete solubilization of DMSO. The absorbance was measured at 540 nm using a microplate reader (Spectra Max ID3; Molecular Devices, San Jose, CA, USA). All data were analyzed using GraphPad Prism 5 (GraphPad Software, La Jolla, CA, USA).

In vitro Clonogenic Assay

HeyA8 cells were seeded in 6-well plates at a density of 200 cells per well and incubated at 37°C for 24 h. After cell adhesion, cells were treated with free fenbendazole, fenbendazole-loaded micelles (M-F), free rapamycin, rapamycin-loaded micelles (M-R), free fenbendazole/rapamycin, or M-FR. The high concentrations treated were 500 nM for free fenbendazole and M-F, 521 nM for free rapamycin and M-R, and 9910 nM for free fenbendazole/rapamycin and M-FR, respectively. After 2 weeks, the medium was removed, and 1 mL of crystal violet (0.5% w/v) was added to each well to stain the colonies. After incubation for 30 min, the 6-well plates were rinsed with clean water. The number of colonies with more than 50 cells was counted. The colony formation percentage was calculated using the following equation below:

$$\text{Colony formation}(\%) = \frac{\text{Number of colonies after treatment}}{\text{Number of colonies of control}} \times 100$$

In vitro Drug Release Assay from Micelles

The release of fenbendazole and rapamycin in micelles was assessed using the dialysis method.[79] A dialysis membrane bag (MWCO 20 kD) containing M-F, M-R, or M-FR was immersed in 2.0 L of phosphate-buffered saline (PBS, pH 7.4). The release medium was stirred at 200 rpm using a magnetic bar at 37°C. Each sample (20 μL) was collected at 0, 2, 4, 6, 24, 48, 72, 168, 240, and 336 h, diluted in 180 μL of ACN, and measured using HPLC. The PBS was replaced with a fresh medium to maintain sink conditions at 8, 24, 72, 168, and 240 h. A curve fitting of % drug release was performed based on the first-order association using GraphPad Prism 8.4.2.[80] All experiments were performed in triplicate.

Animal Care and Development of in vivo Models

This experiment was reviewed and approved by the institutional animal care and use committee (IACUC) of Samsung Biomedical Research Institute (protocol No. H-A9-003), which is an accredited facility by the Association for Assessment and Accreditation of Laboratory Animal Care International (AAALAC) and abides by the Institute of Laboratory Animal Resources (ILAR) guideline. All female BALB/c nude mice used in the experiments were purchased from Orient Bio Inc (Seong-nam, Korea). To establish an orthotopic model, HeyA8 (2.5×10^5 cells/0.1 mL HBSS) cells were injected into the peritoneal cavities of the female BALB/c nude mice.[81] The mice were randomly divided into four groups, and the experiment was conducted at two doses: (i) CON, M-F (2.5 mg/kg), M-R (15 mg/kg), and M-FR (2.5 mg/kg for fenbendazole and 15 mg/kg for rapamycin), (ii) CON, M-F (5 mg/kg), M-R (30 mg/kg), and M-FR (5 mg/kg for fenbendazole and 30 mg/kg for rapamycin). All treatment were IV injected via the tail vein every two days. The mice (n = 10 per group) were monitored daily for tumor development, and sacrificed on days 28–35 after the injection of cancer cells. Body weight, tumor weight, and the number of tumor nodules were recorded. Tumors were fixed in formalin and embedded in paraffin or snap frozen in an optimal cutting temperature compound (Sakura Finetek, Tokyo, Japan) in liquid nitrogen.

Statistical Analysis

Statistical analysis of all data identified significant differences using analysis of variance (ANOVA) with of GraphPad Prism v 5.0. $*p < 0.05$, $**p < 0.01$, and $***p < 0.001$ indicate statistical significance.

Results

Evaluation of the Synergistic Effects of Fenbendazole and Rapamycin in HeyA8 Cells

The optimal ratio of fenbendazole and rapamycin was determined by measuring the 50% inhibition concentration (IC_{50}) values of the two drugs in HeyA8 and analyzing the CI values.[82] IC_{50} values were measured at various molar ratios of fenbendazole and rapamycin (1:1, 1:2, 2:1, 1:4, and 4:1), and the CI values were indicated. The ratio of fenbendazole and rapamycin showing a synergistic effect in HeyA8 cell was confirmed, which became a potential basis for determining the final ratio of the formulation (Table 1 and Figure S1). The inhibitory effect varied depending on the combination ratio that determines the optimal ratio. When the molar ratio was 1:4, CI value > 1, that is, antagonism was observed. All other

Table 1 IC_{50} and CI Values of Fenbendazole and Rapamycin at Various Molar Ratios (n = 3)

Molar Ratio (Fendazole:Rapamycin)	IC_{50} (nM)		CI value
	Fenbendazole	Rapamycin	
1:1	0.10	0.10	0.20
1:2	0.04	0.07	0.11
1:4	0.37	1.46	1.83
2:1	0.57	0.29	0.86
4:1	0.17	0.04	0.21

Abbreviation: CI, combination index.

ratios (1:1, 1:2, 2:1, and 4:1) had CI values of < 1, indicating a synergistic effect. A ratio of 1:2 showed the lowest CI value (Figure S2).

Preparation of M-FR

A micelle was prepared and evaluated, except for the molar ratio of fenbendazole:rapamycin=1:4, in which antagonism appeared. DL (%), EE (%), zeta potential, PDI, and size of M-FR at different ratios (1:1, 1:2, 2:1, and 4:1) were assessed. The PDI and size are listed in Table 2. In the molar ratio of fenbendazole and rapamycin of 1:2, EE (%) of fenbendazole and rapamycin was 75.7 ± 4.61 and 98.0 ± 1.97, respectively. At the molar ratio of 1:1, EE (%) of fenbendazole and rapamycin was 81.5 ± 2.45 and 76.2 ± 8.36, respectively. In contrast, in the ratio of 2:1 and 4:1, the EE (%) of fenbendazole was 40.3 ± 5.17 and 19.5 ± 0.49, respectively, indicating low EE (%). Therefore, considering EE (%), a 1:2 ratio using 100 mg of the mPEG-*b*-PCL polymer was selected as an optimal ratio. The size distribution graph in Figure 2A shows that the vehicle was 30.07 nm, and M-F, M-R, and M-FR were < 30 nm. Also, TEM images showed that the micelles were uniformly spherical (Figure 2B).

Stability Test

The mean size and PDI of M-FR were measured at 4°C and 37°C for 14 days. At 4°C, the mean size was < 50 nm on day 7, and < 80 nm by day 14. During the measurement period, the PDI was < 0.3. At 37°C, the mean size increased to ≥ 200 nm after day 2, and the PDI remained < 0.3 (Figure 3).

Storage Stability Test After Freeze-Drying

Simultaneously encapsulated micelles containing fenbendazole and rapamycin were evaluated for 120 days after freeze-drying. The evaluated physicochemical properties are shown in Table 3. After 1 day after of preparation, the size and PDI of M-FR was 37.5 ± 1.37 nm and 0.23 ± 0.02, respectively. The size and PDI of M-FR after 120 days were 37.4 ± 0.82 nm and 0.21 ± 0.01, respectively. The EE (%) of fenbendazole on days 1 and 120 were 69.7 ± 4.72% and 76.4 ± 12.5%,

Table 2 Physicochemical Properties of M-FR Prepared with Synergistic Drug Ratio (n = 3, Mean ± SD)

Molar Ratio (Fenbendazole: Rapamycin)	Polymer Amount Used (mg)	Encapsulation Efficiency (EE %)		Drug Loading (DL %)		Particle Size (nm)	PolyDispersity Index (PDI)	Zeta Potential (mV)
		Fenbendazole	Rapamycin	Fenbendazole	Rapamycin			
1:1	100	81.5 ± 2.45	76.2 ± 8.36	0.99	3.01	36.9 ± 0.04	0.27 ± 0.01	−1.63 ± 0.59
1:2	100	75.7 ± 4.61	98.0 ± 1.97	0.99	5.66	37.2 ± 1.10	0.20 ± 0.02	−0.07 ± 0.09
2:1	100	40.3 ± 5.17	61.9 ± 4.86	1.96	3.01	37.1 ± 0.41	0.27 ± 0.00	−1.10 ± 1.06
4:1	100	19.5 ± 0.49	59.2 ± 3.83	3.85	3.01	36.5 ± 0.26	0.27 ± 0.01	−0.80 ± 1.00

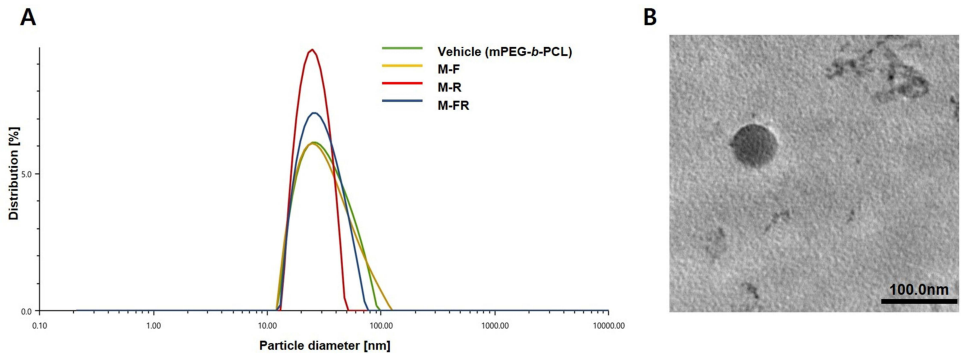

Figure 2 (**A**) Representative size distribution of vehicle, M-F, M-R, and M-FR. (**B**) Transmission electron microscopy (TEM) images of M-FR.
Abbreviations: TEM, Transmission electron microscopy; M-F, fenbendazole-loaded micelle; M-R, rapamycin-loaded micelle; M-FR, fenbendazole/rapamycin-loaded micelle.

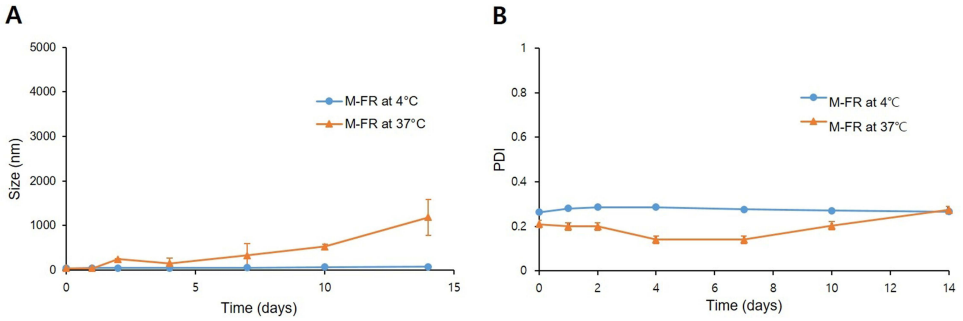

Figure 3 (**A**) Size and (**B**) PDI change in M-FR at 4°C and 37°C (n = 3).
Abbreviations: M-FR, fenbendazole/rapamycin-loaded micelle; PDI, polydispersity index.

respectively. The EE (%) of rapamycin on days 1 and 120 were 96.9 ± 1.65% and 91.6 ± 1.08%, respectively. The zeta potential affects several properties of nano-drug delivery systems.[83] Therefore the zeta potential of M-FR was evaluated, and our formulation was measured to be −0.23 ± 0.13 on day 1 and 0.13 ± 0.19 on day 120. There was no considerable change in the EE (%), size, and zeta potential of M-FR until the last day of evaluation.

Cytotoxicity of M-FR in HeyA8 Cells

Figure 4 shows the cytotoxicity of free fenbendazole, free rapamycin, the final ratio of free fenbendazole/rapamycin, and M-FR. The IC_{50} value of free fenbendazole was 71.6 nM and free rapamycin was 226 nM (Figure 4A and B). The IC_{50} value of free fenbendazole/rapamycin was 14.0 nM, and of the M-FR was 139 nM (Figure 4C and 4D).

Table 3 Long-Term Storage Stability Study of M-FR (n = 3 ± SD)

Days After Freeze-Drying	Encapsulation Efficiency (EE %)		Particle Size (nm)	PolyDispersity Index (PDI)	Zeta Potential (mV)
	Fenbendazole	Rapamycin			
1	69.7 ± 4.72	96.9 ± 1.65	37.5 ± 1.37	0.23 ± 0.02	−0.23 ± 0.13
7	68.1 ± 3.86	97.6 ± 1.97	37.3 ± 0.25	0.24 ± 0.02	−1.10 ± 0.51
14	65.1 ± 8.60	99.3 ± 0.39	42.4 ± 1.35	0.26 ± 0.01	−0.30 ± 0.43
30	65.7 ± 1.09	99.9 ± 0.02	37.6 ± 0.34	0.25 ± 0.01	−1.07 ± 1.44
60	75.7 ± 4.60	96.3 ± 0.75	32.8 ± 0.08	0.15 ± 0.01	−1.13 ± 0.71
120	76.4 ± 12.5	91.6 ± 1.08	37.4 ± 0.82	0.21 ± 0.01	0.13 ± 0.19

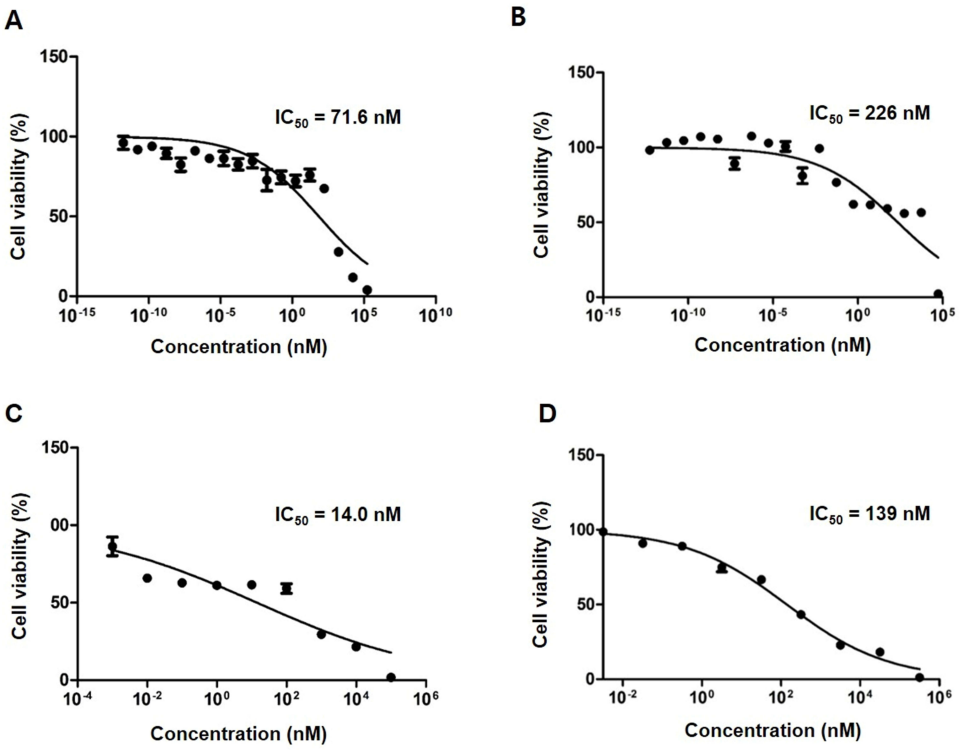

Figure 4 In vitro cytotoxicity assay of HeyA8 cells treated with (**A**) Free fenbendazole, (**B**) Free rapamycin, (**C**) Free fenbendazole/rapamycin, and (**D**) M-FR.
Abbreviations: IC_{50}, 50% inhibition concentration; M-FR, fenbendazole/rapamycin-loaded micelle.

Clonogenic Assay

Clonogenic assays were performed to evaluate the long-term anticancer efficacy of drugs and micelles. Colony formation was compared after 2 weeks of treatment with free fenbendazole, free rapamycin, free fenbendazole/rapamycin, M-F, M-R, or M-FR in HeyA8 cells. For M-F, no colonies were found after 500 nM treatment. Cell viability in the 50 nM and 5 nM treatments was 20.7% and 26.5%, respectively, indicating 1.8-fold and 1.6-fold greater inhibition than free fenbendazole (Figure 5A). For M-R, no colonies were found after 5521 nM treatment, and the colony formation inhibition rate was 1.2 times higher than free rapamycin at 552.1 nM (Figure 5B). For M-FR, no colonies were found after 9910 nM treatment. Treatments with 991 nM and 99.1 nM showed 10-fold and 6.9-fold higher colony formation inhibition than free fenbendazole/rapamycin, respectively, which was statistically significant (***$p < 0.001$) (Figure 5C).

In vitro Drug Release Assay

The release profiles of M-F, M-R and M-FR were evaluated and are shown in Figure 6. The goodness of fit (R^2) and rate constant (k, h^{-1}) based on the first-order are also analyzed. The R^2 and k of fenbendazole calculated from the release

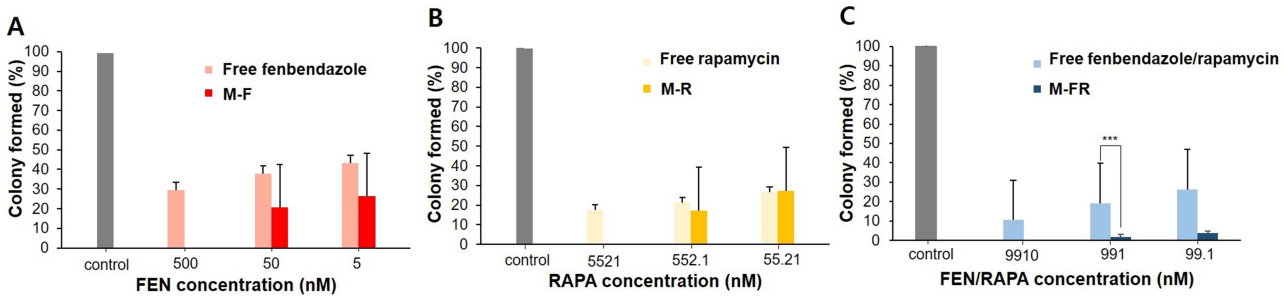

Figure 5 In vitro clonogenic assay results after the treatment of HeyA8 cells with (**A**) Free fenbendazole and M-F, (**B**) Free rapamycin and M-R, and (**C**) Free fenbendazole/rapamycin and M-FR (n = 3).
Abbreviations: M-F, fenbendazole-loaded micelle; M-R, rapamycin-loaded micelle; M-FR, fenbendazole/rapamycin-loaded micelle.

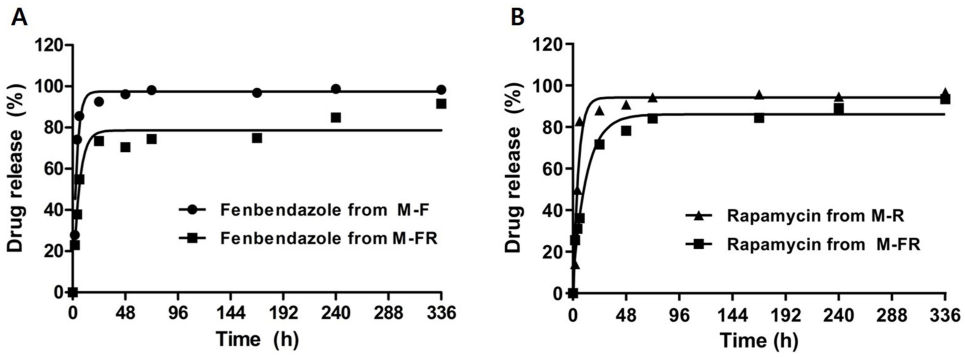

Figure 6 Single and combined drug-release profiles of fenbendazole and rapamycin in micelles. (**A**) Fenbendazole release in M-F and M-FR, and (**B**) Rapamycin release in M-R and M-FR (n = 3).
Abbreviations: M-F, fenbendazole-loaded micelle; M-R, rapamycin-loaded micelle; M-FR, fenbendazole/rapamycin-loaded micelle.

profile were $R^2 = 0.9711$, k = 0.2960 h^{-1} and $R^2 = 0.9568$, k = 0.1795 h^{-1} in M-F and M-FR, respectively. The R^2 and k of rapamycin were $R^2 = 0.9517$, k = 0.2212 h^{-1} and $R^2 = 0.9778$, k = 0.0796 h^{-1} in M-R and M-FR, respectively. For fenbendazole, the release rate was 96.2 ± 1.49% in M-F and 70.4 ± 14.0% in M-FR after 48 h (*p < 0.05). Also, 98.8 ± 0.47% and 84.9 ± 6.29% were released at 240 h, respectively (*p < 0.05). For rapamycin, more than 90% drug was released after 48 h in M-R, but 78.2 ± 7.56% was released in M-FR. Also, 96.7 ± 3.20% and 89.2 ± 7.31% were released at 240 h, respectively.

In vivo Antitumor Efficacy

This experiment was performed twice in the female BALB/c nude mice bearing tumors. Both experiments were divided into the same group (CON, M-F, M-R, and M-FR), and only the dosage was different. Mice from both experiments were observed and injected for 3 weeks, and the sacrifice date and administration interval were also the same (Figure 7A).

In the first experiment, fenbendazole (2.5 mg/kg) and rapamycin (15 mg/kg) were evaluated and expressed as tumor and body weights (Figure 7B and C). The tumor weights of CON and M-FR were 2.09 ± 0.30 g and 0.46 ± 0.17 g, respectively, which were statistically significant (**$p < 0.01$). In addition, no toxicity was observed in any of the groups.

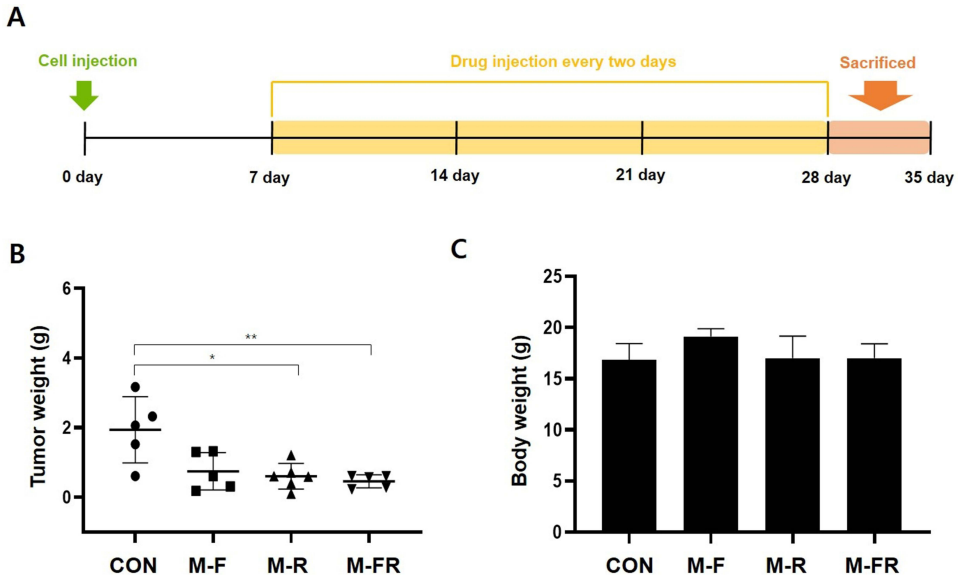

Figure 7 (**A**) Time schedule of antitumor efficacy using a mouse injected with HeyA8 cells, (**B**) Tumor weight when 2.5 mg/kg of fenbendazole and 15 mg/kg of rapamycin were administered, and (**C**) Body weight for toxicity (n = 10). (*$p < 0.05$ and **$p < 0.01$).
Abbreviations: CON, control; M-F, fenbendazole-loaded micelle; M-R, rapamycin-loaded micelle; M-FR, fenbendazole/rapamycin-loaded micelle.

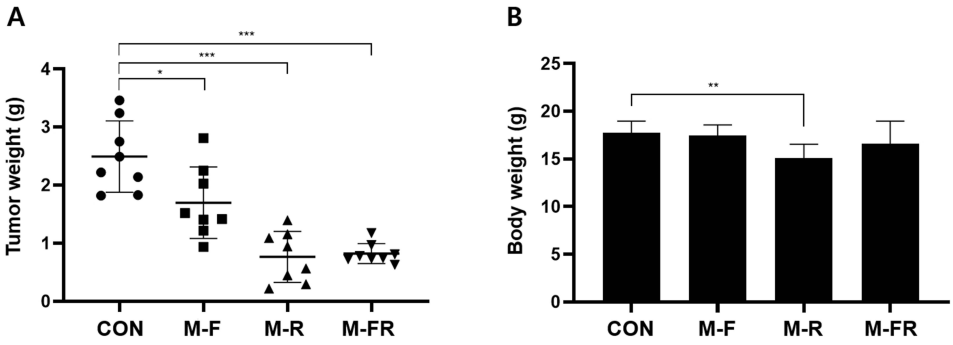

Figure 8 (**A**) Tumor weight when 5 mg/kg of fenbendazole and 30 mg/kg of rapamycin were administered, and (**B**) body weight for toxicity (n = 10). (*p < 0.05, **p< 0.01 and ***p < 0.001).
Abbreviations: CON, control; M-F, fenbendazole-loaded micelle; M-R, rapamycin-loaded micelle; M-FR, fenbendazole/rapamycin-loaded micelle.

In the second experiment, fenbendazole (5 mg/kg) and rapamycin (30 mg/kg) were evaluated and expressed as tumor and body weight (Figure 8A and B). The tumor weight of CON was 2.49 ± 0.58 g, M-R was 0.77 ± 0.41 g, and M-FR was 0.82 ± 0.16 g. Compared with CON, M-R significantly inhibited the tumor (***p < 0.001) but showed toxicity (**p < 0.01). However, M-FR showed a significant antitumor effect (***p < 0.001) and no toxicity.

Discussion

Interfering with microtubule polymerization and inhibiting mTOR signaling are important for OC suppression.[84,85] Therefore, we hypothesized that fenbendazole, which exhibits anticancer activity by interfering with microtubule synthesis, and rapamycin, a mTOR inhibitor, would be effective in OC treatment. Fenbendazole, an anthelmintic drug, has been changed to an anticancer agent and applied to the treatment of OC,[86] and the anticancer potential of mPEG-*b*-PCL micelles encapsulated with fenbendazole and rapamycin has been reported.[74] Therefore, we evaluated the optimal ratio of the two drugs required for exhibiting a synergistic effect by obtaining CI values in HeyA8 cells, an OC cell line.[77,87] Although synergism was observed at various molar ratios of fenbendazole and rapamycin, the EE (%) of fenbendazole was significantly lower as <50% at 2:1 and 4:1. The EE (%) of 1:1 and 1:2 were >70%,[88] and the size and PDI of the two ratios were < 40 nm and 0.3, respectively. Therefore, M-FR can be expected to accumulate more in tumors than in normal tissues through the EPR effect.[89–91] Fabricating micelles using a 1:2 molar ratio of fenbendazole: rapamycin with high EE (%) and small size and synergistic effect is the most suitable.

In this study, we evaluated whether micelles could be stored for a long time. Freeze-drying is a suitable technique for improving the long-term stability of colloidal nanoparticles.[92] Our formulation was stored at −20°C and evaluated for up to 120 days. No significant difference in physicochemical properties was observed from day 1. Therefore, we recommend long-term storage of the formulation at −20°C. In addition, M-FR in an aqueous solution were observed at 4°C and 37°C for 2 weeks. At 4°C, day 7 showed 51.9 ± 3.36 nm, and <90 nm was maintained until day 14. Therefore, it is recommended to store at 4°C to maintain the stability of M-FR in a liquid state. On the other hand, the size gradually increased from the day 1 at 37°C, and the PDI was maintained at <0.3 until 14 days.[93]

In the evaluation of in vitro cytotoxicity by the MTT assay, the IC_{50} value of free fenbendazole/rapamycin was lesser than of M-FR, possibly because the micelles delay drug release.[15] Also, the drug encapsulated in micelles was released more slowly than 48 h (drug treatment time in MTT assay), indicating the cytotoxic effect of the drug may be lower than that of the free drug.[94] In the clonogenic assay, the colony formation inhibition rate of fenbendazole and rapamycin was evaluated for 14 days. The clonogenic assay evaluates the rate of colonial formation inhibition over a longer period than the MTT assay.[95] As a result, the cell viability treated with 991 nM M-FR was 1.91%, showing a significant difference by inhibiting colonies by 6.9 times compared to the treatment with free fenbendazole/rapamycin at the same concentration (***p < 0.001).

The release rate of fenbendazole was compared in M-F and M-FR, and the release of rapamycin in M-R and M-FR. At 6 h, rapamycin was released > 80% in M-R but 36.2 ± 16.6% in M-FR. In addition, rapamycin release of more than 90% was observed at 48 h in M-R and 336 h in M-FR. At 48 h, fenbendazole was released by 96.2 ± 1.49% and 70.4 ±

14.0% in M-F and M-FR, respectively, indicating a statistically significant difference (*p < 0.05). In addition, 98.8 ± 0.47% and 84.9 ± 6.29% of fenbendazole in M-F and M-FR at 240 h showed a significant difference in release (*p < 0.05). Comparing the release of fenbendazole from combination micelles and single micelles, a significant difference was found at the two time points, suggesting that hydrophobic drug-drug interactions probably occurred in the micelle core.[96] No explosive release initially in M-FR, indicates the possibility of preventing the explosive release of high-dose drugs,[97] which, in turn, can prevent toxicity in the body.

The first evaluation of in vivo antitumor efficacy (2.5 mg/kg fenbendazole, 15 mg/kg rapamycin), showed that M-FR had a significant antitumor effect compared to the CON (**$p < 0.01$). However, when M-F and M-R were compared with M-FR, there was no significant difference. We doubled the dose of each drug in the second step considering no toxicity was found in any group. In the second evaluation, only M-R showed toxicity (**$p < 0.01$), and no toxicity observed in M-F. These results are attributed to the selective toxicity of fenbendazole to tumor cells and its high stability in vivo.[98,99] Nevertheless, in vivo anticancer evaluation indicates that M-FR does not significantly inhibit cancer cells compared with M-FR, probably due to the loss of carrier or drug after injection, as in vivo anticancer evaluations are performed in complex structures, unlike in vitro cytotoxicity tests.[100,101] Therefore, M-FR may not have reached the tumor or M-FR may not have reached the tumor at this designated ratio. However, in the two in vivo antitumor efficacy evaluations, M-FR showed a significant antitumor effect compared with CON (**$p < 0.01$, ***$p < 0.001$) and no toxicity was observed.

Compare with rapamycin, fenbendazole did not enhance the anticancer effect of M-FR compared to rapamycin. This result may be due to insufficient fenbendazole dose; however, owing to its low solubility,[102] encapsulating a high dose of fenbendazole was not possible. Further studies are required to increase and improve the capacity of fenbendazole in other systems to make it a useful combination.

Conclusions

We evaluated the ability of micelles encapsulated with fenbendazole and the mTOR inhibitor, rapamycin, to prevent microtubule polymerization in OC. Various ratios of drug combinations were evaluated in OC cells, and synergistic effects were observed in many combination ratios. After evaluating the physicochemical properties of the formulation prepared at a ratio showing a synergistic effect, an optimal formulation ratio of 1:2 was obtained. In an in vitro study, M-FR showed higher colony inhibition than the free drug and released the drug relatively slower than M-F and M-R. Formulations designed for the two doses were evaluated by establishing a HeyA8 orthotopic model for in vivo antitumor efficacy. M-FR significantly inhibited OC compared to CON, and M-FR was not toxic at either dose tested. Therefore, we believe that the application of other polymers may result in a better formulation. We hope that this study will help future research on fenbendazole and rapamycin researchers.

Abbreviations

OC, ovarian cancer; EOC, epithelial ovarian cancer; EPR, enhanced permeability and retention; mPEG-*b*-PCL, methoxy poly(ethylene glycol)-*b*-poly(caprolactone); mTOR, mammalian target of rapamycin; IV, intravenous; ACN, acetonitrile; HBSS, Hank's balanced salt solution; DW, distilled water; MTT, thiazolyl blue tetrazolium bromide; DMSO, dimethyl sulfoxide; HPLC, high-performance liquid chromatography; FBS, fetal bovine serum; RPMI, Roswell Park Memorial Institute; DPBS, Dulbecco's phosphate-buffered saline; M-FR, fenbendazole/rapamycin-loaded mPEG-*b*-PCL micelle; PDI, polydispersity index; DLS, dynamic light scattering; EE, encapsulation efficiency; DL, drug loading; CI, combination index; M-F, fenbendazole-loaded micelle; M-R, rapamycin-loaded micelle; PBS, phosphate-buffered saline; IACUC, Institutional Animal Care and Use Committee; AAALAC, Association for Assessment and Accreditation of Laboratory Resources; ILAR, Institute of Laboratory Animal Resources; IC_{50}, 50% inhibition concentration.

Data Sharing Statement

All the data contained in the article is available upon request.

Ethics Approval

This experiment was reviewed and approved by the institutional animal care and use committee (IACUC) of Samsung Biomedical Research Institute (protocol No. H-A9-003), which is an accredited facility by the Association for Assessment and Accreditation of Laboratory Animal Care International (AAALAC) and abides by the Institute of Laboratory Animal Resources (ILAR) guideline.

Author Contributions

Conceptualization, Y.B.S., D.H.S., and J.W.L.; methodology, Y.B.S. and J.Y.C.; software, Y.B.S.; validation, Y.B.S. and D.H.S.; formal analysis, Y.B.S. and J.Y.C; investigation, Y.B.S. and J.Y.C; resources, D.H.S and J.W.L; data curation, Y.B.S., J.Y.C., D.H.S., and J.W.L.; interpretation, Y.B.S., J.Y.C., D.H.S., and J.W.L.; writing-original draft preparation, Y.B.S.; writing-review and editing, Y.B.S., J.Y.C., D.H.S., and J.W.L.; visualization, Y.B.S., super-vision, D.H.S. and J.W.L; project administration, Y.B.S., J.Y.C., D.H.S., and J.W.L. All authors made substantial contributions to conception and design, acquisition of data, or analysis and interpretation of data; took part in drafting the article or revising it critically for important intellectual content; agreed to submit to the current journal; gave final approval of the version to be published; and agree to be accountable for all aspects of the work.

Funding

This research was supported by "Regional Innovation Strategy (RIS)" through the National Research Foundation of Korea (NRF) funded by the Ministry of Education (MOE) (2021RIS-001). It is also supported by National Research Foundation (NRF) of Korea Grand funded by the Korean government (MSIP) grant [MRC2017R1A5A2015541] and the Basic Science Research Program through National Research Foundation of Korea (NRF), funded by the Ministry of Education (MOE), grant [NRF-2022R1C1C1007107].

Disclosure

Yu Been Shin and Ju-Yeon Choi are co-first authors for this study. The authors report no conflicts of interest in this work.

References

1. Stewart C, Ralyea C, Lockwood S. Ovarian cancer: an integrated review. *Semin Oncol Nurs*. 2019;35(2):151–156. doi:10.1016/j.soncn.2019.02.001
2. Shim SH, Lim MC, Lee D, et al. Cause-specific mortality rate of ovarian cancer in the presence of competing risks of death: a nationwide population-based cohort study. *J Gynecol Oncol*. 2022;33(1):e5. doi:10.3802/jgo.2022.33.e5
3. Reid BM, Permuth JB, Sellers TA. Epidemiology of ovarian cancer: a review. *Cancer Biol Med*. 2017;14(1):9–32. doi:10.20892/j.issn.2095-3941.2016.0084
4. Assi S, Barling M, Al-Hamid A, Cheema E. Exploring the adverse effects of chemotherapeutic agents used in the treatment of cervical and ovarian cancer from the patients' perspective: a content analysis of the online discussion forums. *Eur J Hosp Pharm*. 2021;28(Suppl 2):e35–e40. doi:10.1136/ejhpharm-2019-002162
5. Ng JS, Low JJ, Ilancheran A. Epithelial ovarian cancer. *Best Pract Res Clin Obstet Gynaecol*. 2012;26(3):337–345. doi:10.1016/j.bpobgyn.2011.12.005
6. González-Martín A, Pothuri B, Vergote I, et al. Niraparib in patients with newly diagnosed advanced ovarian cancer. *N Engl J Med*. 2019;381(25):2391–2402. doi:10.1056/NEJMoa1910962
7. Miller EM, Samec TM, Alexander-Bryant AA. Nanoparticle delivery systems to combat drug resistance in ovarian cancer. *Nanomedicine*. 2021;31:102309. doi:10.1016/j.nano.2020.102309
8. Alexis F, Rhee J-W, Richie JP, Radovic-Moreno AF, Langer R, Farokhzad OC. New frontiers in nanotechnology for cancer treatment. Paper presented at: Urologic Oncology: Seminars and Original Investigations; 2008.
9. Qaiser A, Kiani MH, Parveen R, et al. Design and synthesis of multifunctional polymeric micelles for targeted delivery in Helicobacter pylori infection. *J Mol Liq*. 2022;363:119802. doi:10.1016/j.molliq.2022.119802
10. Razzaq S, Rauf A, Raza A, et al. A multifunctional polymeric micelle for targeted delivery of paclitaxel by the inhibition of the P-Glycoprotein transporters. *Nanomaterials*. 2021;11(11):2858. doi:10.3390/nano11112858
11. Kiani MH, Ul hassan MR, Hussain S, et al. Cholesterol decorated thiolated stereocomplexed nanomicelles for improved anti-mycobacterial potential via efflux pump and mycothione reductase inhibition. *J Mol Liq*. 2022;367:120378. doi:10.1016/j.molliq.2022.120378
12. Kipp JE. The role of solid nanoparticle technology in the parenteral delivery of poorly water-soluble drugs. *Int J Pharm*. 2004;284(1–2):109–122. doi:10.1016/j.ijpharm.2004.07.019
13. Zhang L, Chan JM, Gu FX, et al. Self-assembled lipid--polymer hybrid nanoparticles: a robust drug delivery platform. *ACS nano*. 2008;2(8):1696–1702. doi:10.1021/nn800275r

14. Stroh M, Zimmer JP, Duda DG, et al. Quantum dots spectrally distinguish multiple species within the tumor milieu in vivo. *Nat Med*. 2005;11(6):678–682. doi:10.1038/nm1247
15. Woo HN, Chung HK, Ju EJ, et al. Preclinical evaluation of injectable sirolimus formulated with polymeric nanoparticle for cancer therapy. *Int J Nanomedicine*. 2012;7:2197. doi:10.2147/IJN.S29480
16. Rahdar A, Hasanein P, Bilal M, Beyzaei H, Kyzas GZ. Quercetin-loaded F127 nanomicelles: antioxidant activity and protection against renal injury induced by gentamicin in rats. *Life Sci*. 2021;276:119420. doi:10.1016/j.lfs.2021.119420
17. Alexis F, Pridgen E, Molnar LK, Farokhzad OC. Factors affecting the clearance and biodistribution of polymeric nanoparticles. *Mol Pharm*. 2008;5(4):505–515. doi:10.1021/mp800051m
18. Miller MA, Zheng YR, Gadde S, et al. Tumour-associated macrophages act as a slow-release reservoir of nano-therapeutic Pt(IV) pro-drug. *Nat Commun*. 2015;6:8692. doi:10.1038/ncomms9692
19. Miller MA, Gadde S, Pfirschke C, et al. Predicting therapeutic nanomedicine efficacy using a companion magnetic resonance imaging nanoparticle. *Sci Transl Med*. 2015;7(314):314ra183. doi:10.1126/scitranslmed.aac6522
20. Levit SL, Tang C. Polymeric nanoparticle delivery of combination therapy with synergistic effects in ovarian cancer. *Nanomaterials*. 2021;11(4):1048. doi:10.3390/nano11041048
21. Rahdar A, Kazemi S, Askari F. Pluronic as nano-carrier for drug delivery systems. *Nanomed Res J*. 2018;3(4):174–179.
22. Maeda H, Wu J, Sawa T, Matsumura Y, Hori K. Tumor vascular permeability and the EPR effect in macromolecular therapeutics: a review. *J Control Release*. 2000;65(1–2):271–284. doi:10.1016/S0168-3659(99)00248-5
23. Maeda H. Toward a full understanding of the EPR effect in primary and metastatic tumors as well as issues related to its heterogeneity. *Adv Drug Deliv Rev*. 2015;91:3–6. doi:10.1016/j.addr.2015.01.002
24. Danhier F. To exploit the tumor microenvironment: since the EPR effect fails in the clinic, what is the future of nanomedicine? *J Control Release*. 2016;244(Pt A):108–121. doi:10.1016/j.jconrel.2016.11.015
25. Shi Y, van der Meel R, Chen X, Lammers T. The EPR effect and beyond: strategies to improve tumor targeting and cancer nanomedicine treatment efficacy. *Theranostics*. 2020;10(17):7921–7924. doi:10.7150/thno.49577
26. Sun H, Yang R, Wang J, et al. Component-based biocompatibility and safety evaluation of polysorbate 80. *RSC Adv*. 2017;7(25):15127–15138. doi:10.1039/C6RA27242H
27. Hu X-J, Liu Y, Zhou X-F, et al. Synthesis and characterization of low-toxicity N-caprinoyl-N-trimethyl chitosan as self-assembled micelles carriers for osthole. *Int J Nanomedicine*. 2013;8:3543. doi:10.2147/IJN.S46369
28. Sinha VR, Bansal K, Kaushik R, Kumria R, Trehan A. Poly-epsilon-caprolactone microspheres and nanospheres: an overview. *Int J Pharm*. 2004;278(1):1–23. doi:10.1016/j.ijpharm.2004.01.044
29. Chawla JS, Amiji MM. Biodegradable poly(epsilon -caprolactone) nanoparticles for tumor-targeted delivery of tamoxifen. *Int J Pharm*. 2002;249(1–2):127–138. doi:10.1016/S0378-5173(02)00483-0
30. Ali ME, Lamprecht A. Polyethylene glycol as an alternative polymer solvent for nanoparticle preparation. *Int J Pharm*. 2013;456(1):135–142. doi:10.1016/j.ijpharm.2013.07.077
31. Kumari A, Yadav SK, Yadav SC. Biodegradable polymeric nanoparticles based drug delivery systems. *Colloids Surf B Biointerfaces*. 2010;75(1):1–18. doi:10.1016/j.colsurfb.2009.09.001
32. Wei X, Gong C, Gou M, et al. Biodegradable poly (ε-caprolactone)–poly (ethylene glycol) copolymers as drug delivery system. *Int J Pharm*. 2009;381(1):1–18. doi:10.1016/j.ijpharm.2009.07.033
33. Gou M, Wei X, Men K, et al. PCL/PEG copolymeric nanoparticles: potential nanoplatforms for anticancer agent delivery. *Curr Drug Targets*. 2011;12(8):1131–1150. doi:10.2174/138945011795906642
34. Al-Lazikani B, Banerji U, Workman P. Combinatorial drug therapy for cancer in the post-genomic era. *Nat Biotechnol*. 2012;30(7):679–692. doi:10.1038/nbt.2284
35. Bansal M, Yang J, Karan C, et al. A community computational challenge to predict the activity of pairs of compounds. *Nat Biotechnol*. 2014;32(12):1213–1222. doi:10.1038/nbt.3052
36. Khdair A, Chen D, Patil Y, et al. Nanoparticle-mediated combination chemotherapy and photodynamic therapy overcomes tumor drug resistance. *J Control Release*. 2010;141(2):137–144. doi:10.1016/j.jconrel.2009.09.004
37. Blagosklonny MV. Overcoming limitations of natural anticancer drugs by combining with artificial agents. *Trends Pharmacol Sci*. 2005;26(2):77–81. doi:10.1016/j.tips.2004.12.002
38. Muser RK, Paul JW. Safety of fenbendazole use in cattle. *Mod Vet Pract*. 1984;65(5):371–374.
39. Schwartz RD, Donoghue AR, Baggs RB, Clark T, Partington C. Evaluation of the safety of fenbendazole in cats. *Am J Vet Res*. 2000;61(3):330–332. doi:10.2460/ajvr.2000.61.330
40. Hayes RH, Oehme FW, Leipold H. Safety of fenbendazole in swine. *Am J Vet Res*. 1983;44(6):1112–1116.
41. Short CR, Flory W, Hsieh LC, Barker SA. The oxidative metabolism of fenbendazole: a comparative study. *J Vet Pharmacol Ther*. 1988;11(1):50–55. doi:10.1111/j.1365-2885.1988.tb00120.x
42. Schiff PB, Horwitz SB. Taxol stabilizes microtubules in mouse fibroblast cells. *Proc Natl Acad Sci U S A*. 1980;77(3):1561–1565. doi:10.1073/pnas.77.3.1561
43. Lai SR, Castello SA, Robinson AC, Koehler JW. In vitro anti-tubulin effects of mebendazole and fenbendazole on canine glioma cells. *Vet Comp Oncol*. 2017;15(4):1445–1454. doi:10.1111/vco.12288
44. Dawson PJ, Gutteridge WE, Gull K. A comparison of the interaction of anthelmintic benzimidazoles with tubulin isolated from mammalian tissue and the parasitic nematode Ascaridia galli. *Biochem Pharmacol*. 1984;33(7):1069–1074. doi:10.1016/0006-2952(84)90515-X
45. Dogra N, Kumar A, Mukhopadhyay T. Fenbendazole acts as a moderate microtubule destabilizing agent and causes cancer cell death by modulating multiple cellular pathways. *Sci Rep*. 2018;8(1):1–15. doi:10.1038/s41598-018-30158-6
46. Dogra N, Mukhopadhyay T. Impairment of the ubiquitin-proteasome pathway by methyl N-(6-phenylsulfanyl-1H-benzimidazol-2-yl)carbamate leads to a potent cytotoxic effect in tumor cells: a novel antiproliferative agent with a potential therapeutic implication. *J Biol Chem*. 2012;287(36):30625–30640. doi:10.1074/jbc.M111.324228
47. Nosengo N. Can you teach old drugs new tricks? *Nature*. 2016;534(7607):314–316. doi:10.1038/534314a

48. Park D. Fenbendazole suppresses growth and induces apoptosis of actively growing H4IIE hepatocellular carcinoma cells via p21-mediated cell-cycle arrest. *Biol Pharm Bull*. 2022;45(2):184–193. doi:10.1248/bpb.b21-00697
49. Duan Q, Liu Y, Rockwell S. Fenbendazole as a potential anticancer drug. *Anticancer Res*. 2013;33(2):355–362.
50. Mukhopadhyay T, Sasaki J-I, Ramesh R, Roth JA. Mebendazole elicits a potent antitumor effect on human cancer cell lines both in vitro and in vivo. *Clin Cancer Res*. 2002;8(9):2963–2969.
51. Spagnuolo PA, Hu J, Hurren R, et al. The antihelmintic flubendazole inhibits microtubule function through a mechanism distinct from Vinca alkaloids and displays preclinical activity in leukemia and myeloma. *Blood*. 2010;115(23):4824–4833.
52. Martarelli D, Pompei P, Baldi C, Mazzoni G. Mebendazole inhibits growth of human adrenocortical carcinoma cell lines implanted in nude mice. *Cancer Chemother Pharmacol*. 2008;61(5):809–817. doi:10.1007/s00280-007-0538-0
53. Short CR, Barker SA, Hsieh LC, Ou SP, McDowell T. Disposition of fenbendazole in the rabbit. *Res Vet Sci*. 1988;44(2):215–219. doi:10.1016/S0034-5288(18)30842-7
54. McKellar QA, Harrison P, Galbraith EA, Inglis H. Pharmacokinetics of fenbendazole in dogs. *J Vet Pharmacol Ther*. 1990;13(4):386–392. doi:10.1111/j.1365-2885.1990.tb00793.x
55. Martel RR, Klicius J, Galet S. Inhibition of the immune response by rapamycin, a new antifungal antibiotic. *Can J Physiol Pharmacol*. 1977;55(1):48–51. doi:10.1139/y77-007
56. Guba M, von Breitenbuch P, Steinbauer M, et al. Rapamycin inhibits primary and metastatic tumor growth by antiangiogenesis: involvement of vascular endothelial growth factor. *Nat Med*. 2002;8(2):128–135. doi:10.1038/nm0202-128
57. Viñals F, Chambard JC, Pouysségur J. p70 S6 kinase-mediated protein synthesis is a critical step for vascular endothelial cell proliferation. *J Biol Chem*. 1999;274(38):26776–26782. doi:10.1074/jbc.274.38.26776
58. Rowinsky EK. Targeting the molecular target of rapamycin (mTOR). *Curr Opin Oncol*. 2004;16(6):564–575. doi:10.1097/01.cco.0000143964.74936.d1
59. Tengku Din TA, Seeni A, Khairi WN, Shamsuddin S, Jaafar H. Effects of rapamycin on cell apoptosis in MCF-7 human breast cancer cells. *Asian Pac J Cancer Prev*. 2014;15(24):10659–10663. doi:10.7314/APJCP.2014.15.24.10659
60. Hara K, Maruki Y, Long X, et al. Raptor, a binding partner of target of rapamycin (TOR), mediates TOR action. *Cell*. 2002;110(2):177–189. doi:10.1016/S0092-8674(02)00833-4
61. Kim DH, Sarbassov DD, Ali SM, et al. mTOR interacts with raptor to form a nutrient-sensitive complex that signals to the cell growth machinery. *Cell*. 2002;110(2):163–175. doi:10.1016/S0092-8674(02)00808-5
62. Hennessy BT, Smith DL, Ram PT, Lu Y, Mills GB. Exploiting the PI3K/AKT pathway for cancer drug discovery. *Nat Rev Drug Discov*. 2005;4(12):988–1004. doi:10.1038/nrd1902
63. Mabuchi S, Kuroda H, Takahashi R, Sasano T. The PI3K/AKT/mTOR pathway as a therapeutic target in ovarian cancer. *Gynecol Oncol*. 2015;137(1):173–179. doi:10.1016/j.ygyno.2015.02.003
64. Liang S, Yang N, Pan Y, et al. Expression of activated PIK3CA in ovarian surface epithelium results in hyperplasia but not tumor formation. *PLoS One*. 2009;4(1):e4295. doi:10.1371/journal.pone.0004295
65. Wu R, Hu TC, Rehemtulla A, Fearon ER, Cho KR. Preclinical testing of PI3K/AKT/mTOR signaling inhibitors in a mouse model of ovarian endometrioid adenocarcinomaPI3K/AKT/mTOR inhibitors in an ovarian cancer model. *Clin Cancer Res*. 2011;17(23):7359–7372. doi:10.1158/1078-0432.CCR-11-1388
66. Montero JC, Chen X, Ocaña A, Pandiella A. Predominance of mTORC1 over mTORC2 in the regulation of proliferation of ovarian cancer cells: therapeutic implicationsmTOR targeting in ovarian cancer. *Mol Cancer Ther*. 2012;11(6):1342–1352. doi:10.1158/1535-7163.MCT-11-0723
67. Zhou Q, Wong CH, Lau CPY, et al. Enhanced antitumor activity with combining effect of mTOR inhibition and microtubule stabilization in hepatocellular carcinoma. *Int J Hepatol*. 2013;2013:1–10. doi:10.1155/2013/103830
68. Napoli KL, Wang ME, Stepkowski SM, Kahan BD. Distribution of sirolimus in rat tissue. *Clin Biochem*. 1997;30(2):135–142. doi:10.1016/S0009-9120(96)00157-9
69. Simamora P, Alvarez JM, Yalkowsky SH. Solubilization of rapamycin. *Int J Pharm*. 2001;213(1–2):25–29. doi:10.1016/S0378-5173(00)00617-7
70. Zhang Y, Huang Y, Li S. Polymeric micelles: nanocarriers for cancer-targeted drug delivery. *AAPS PharmSciTech*. 2014;15(4):862–871. doi:10.1208/s12249-014-0113-z
71. Liu X, Zhou H, Yu W, Xiong X, Krastev R, Ma X. Preparation of cationic amphiphilic nanoparticles with modified chitosan derivatives for doxorubicin delivery. *Material*. 2021;14(22):7010. doi:10.3390/ma14227010
72. Chen MC, Tsai HW, Liu CT, et al. A nanoscale drug-entrapment strategy for hydrogel-based systems for the delivery of poorly soluble drugs. *Biomaterials*. 2009;30(11):2102–2111. doi:10.1016/j.biomaterials.2008.12.047
73. Lu W, Li F, Mahato RI. Poly(ethylene glycol)-block-poly(2-methyl-2-benzoxycarbonyl-propylene carbonate) micelles for rapamycin delivery: in vitro characterization and biodistribution. *J Pharm Sci*. 2011;100(6):2418–2429. doi:10.1002/jps.22467
74. Shin HJ, Jo MJ, Jin IS, Park C-W, Kim J-S, Shin DH. Optimization and pharmacokinetic evaluation of synergistic fenbendazole and rapamycin co-encapsulated in methoxy poly (ethylene glycol)-b-poly (caprolactone) polymeric micelles. *Int J Nanomedicine*. 2021;16:4873. doi:10.2147/IJN.S315782
75. Sun C, Liang Y, Hao N, et al. A ROS-responsive polymeric micelle with a π-conjugated thioketal moiety for enhanced drug loading and efficient drug delivery. *Org Biomol Chem*. 2017;15(43):9176–9185. doi:10.1039/C7OB01975K
76. Zhang W, Li C, Jin Y, et al. Multiseed liposomal drug delivery system using micelle gradient as driving force to improve amphiphilic drug retention and its anti-tumor efficacy. *Drug Deliv*. 2018;25(1):611–622. doi:10.1080/10717544.2018.1440669
77. Chou T-C. Drug combination studies and their synergy quantification using the chou-talalay methodsynergy quantification method. *Cancer Res*. 2010;70(2):440–446. doi:10.1158/0008-5472.CAN-09-1947
78. Meerloo JV, Kaspers GJ, Cloos J. Cell sensitivity assays: the MTT assay. In: *Cancer Cell Culture*. Springer; 2011:237–245.
79. Modi S, Anderson BD. Determination of drug release kinetics from nanoparticles: overcoming pitfalls of the dynamic dialysis method. *Mol Pharm*. 2013;10(8):3076–3089. doi:10.1021/mp400154a

80. Schwartz JB, Simonelli AP, Higuchi WI. Drug release from wax matrices I. Analysis of data with first-order kinetics and with the diffusion-controlled model. *J Pharm Sci*. 1968;57(2):274–277. doi:10.1002/jps.2600570206
81. Kim J, Cho YJ, Ryu JY, et al. CDK7 is a reliable prognostic factor and novel therapeutic target in epithelial ovarian cancer. *Gynecol Oncol*. 2020;156(1):211–221. doi:10.1016/j.ygyno.2019.11.004
82. Zhang RX, Wong HL, Xue HY, Eoh JY, Wu XY. Nanomedicine of synergistic drug combinations for cancer therapy – strategies and perspectives. *J Control Release*. 2016;240:489–503. doi:10.1016/j.jconrel.2016.06.012
83. Honary S, Zahir F. Effect of zeta potential on the properties of nano-drug delivery systems-a review (Part 1). *Trop J Pharm Res*. 2013;12 (2):255–264.
84. Dobbin ZC, Landen CN. The importance of the PI3K/AKT/MTOR pathway in the progression of ovarian cancer. *Int J Mol Sci*. 2013;14 (4):8213–8227. doi:10.3390/ijms14048213
85. Tymon-Rosario J, Adjei NN, Roque DM, Santin AD. Microtubule-interfering drugs: current and future roles in epithelial ovarian cancer treatment. *Cancers*. 2021;13(24):6239. doi:10.3390/cancers13246239
86. Elayapillai S, Ramraj S, Benbrook DM, et al. Potential and mechanism of mebendazole for treatment and maintenance of ovarian cancer. *Gynecol Oncol*. 2021;160(1):302–311. doi:10.1016/j.ygyno.2020.10.010
87. Chou T-C. The mass-action law based algorithm for cost-effective approach for cancer drug discovery and development. *Am J Cancer Res*. 2011;1(7):925. doi:10.1039/C0IB00130a
88. Sahu A, Kasoju N, Goswami P, Bora U. Encapsulation of curcumin in pluronic block copolymer micelles for drug delivery applications. *J Biomater Appl*. 2011;25(6):619–639. doi:10.1177/0885328209357110
89. Fang J, Islam W, Maeda H. Exploiting the dynamics of the EPR effect and strategies to improve the therapeutic effects of nanomedicines by using EPR effect enhancers. *Adv Drug Deliv Rev*. 2020;157:142–160. doi:10.1016/j.addr.2020.06.005
90. Torchilin V. Tumor delivery of macromolecular drugs based on the EPR effect. *Adv Drug Deliv Rev*. 2011;63(3):131–135. doi:10.1016/j.addr.2010.03.011
91. Maeda H. Polymer therapeutics and the EPR effect. *J Drug Target*. 2017;25(9–10):781–785. doi:10.1080/1061186X.2017.1365878
92. Chacon M, Molpeceres J, Berges L, Guzman M, Aberturas M. Stability and freeze-drying of cyclosporine loaded poly (D, L lactide–glycolide) carriers. *Eur J Pharm Sci*. 1999;8(2):99–107. doi:10.1016/S0928-0987(98)00066-9
93. Öztürk K, Arslan FB, Öztürk SC, Çalış S. Mixed micelles formulation for carvedilol delivery: in-vitro characterization and in-vivo evaluation. *Int J Pharm*. 2022;611:121294. doi:10.1016/j.ijpharm.2021.121294
94. Zeng X, Zhang Y, Nyström AM. Endocytic uptake and intracellular trafficking of bis-MPA-based hyperbranched copolymer micelles in breast cancer cells. *Biomacromolecules*. 2012;13(11):3814–3822. doi:10.1021/bm301281k
95. Plumb JA. Cell sensitivity assays: clonogenic assay. In: *Cancer Cell Culture*. Springer; 2004:159–164.
96. Wan X, Beaudoin JJ, Vinod N, et al. Co-delivery of paclitaxel and cisplatin in poly (2-oxazoline) polymeric micelles: implications for drug loading, release, pharmacokinetics and outcome of ovarian and breast cancer treatments. *Biomaterials*. 2019;192:1–14. doi:10.1016/j.biomaterials.2018.10.032
97. Senapati S, Mahanta AK, Kumar S, Maiti P. Controlled drug delivery vehicles for cancer treatment and their performance. *Signal Transduct Target Ther*. 2018;3(1):1–19. doi:10.1038/s41392-017-0004-3
98. Villar D, Cray C, Zaias J, Altman NH. Biologic effects of fenbendazole in rats and mice: a review. *J Am Assoc Lab Anim Sci*. 2007;46(6):8–15.
99. Son DS, Lee ES, Adunyah SE. The antitumor potentials of benzimidazole anthelmintics as repurposing drugs. *Immune Netw*. 2020;20(4):e29. doi:10.4110/in.2020.20.e29
100. Ruenraroengsak P, Cook JM, Florence AT. Nanosystem drug targeting: facing up to complex realities. *J Control Release*. 2010;141(3):265–276. doi:10.1016/j.jconrel.2009.10.032
101. Sayes CM, Reed KL, Warheit DB. Assessing toxicity of fine and nanoparticles: comparing in vitro measurements to in vivo pulmonary toxicity profiles. *Toxicol Sci*. 2007;97(1):163–180. doi:10.1093/toxsci/kfm018
102. Petersen MB, Friis C. Pharmacokinetics of fenbendazole following intravenous and oral administration to pigs. *Am J Vet Res*. 2000;61 (5):573–576. doi:10.2460/ajvr.2000.61.573